Repeated loss of variation in insect ovary morphology highlights the role of development in life-history evolution - Supplementary Methods

Samuel H. Church[1]*, Bruno A. S. De Medeiros[1,2], Seth Donoughe[1,3], Nicole L. Márquez Reyes[4], Cassandra G. Extavour[1,5]*

Contents

[1] Department of Organismic and Evolutionary Biology, Harvard University, Cambridge, MA 02138, USA

[2] Smithsonian Tropical Research Institute, Panama City, Panama

[3] Department of Molecular Genetics and Cell Biology, University of Chicago, Chicago, IL 60637, USA

[4] Department of Biology, Universidad de Puerto Rico en Cayey, Cayey 00736, PR

[5] Department of Molecular & Cellular Biology, Harvard University, Cambridge, MA 02138, USA

* Corresponding author

Contents

1 Gathering ovariole number records

We searched the published literature for references to insect ovariole number using a predetermined set of 131 search terms, entered into Google Scholar (scholar.google.com) between June and October of 2019. Each search term consisted of an insect taxonomic group and the words "ovariole number". This list was created to include all insect orders, many large insect families, and groups well-represented in the insect egg dataset. The list of search terms is available in the supplementary file 'ovariole_number_search_terms.tsv'.

For each search term, we evaluated all publications in the first page of results (ten publications). For 61 search terms that had a large number of informative hits, significant representation in the egg dataset, or that corresponded to very speciose groups, we evaluated an additional 20 publications. If a publication reported ovariole number for one or more insect species, we recorded the following information: (1) genus, (2) species name, when available, (3) taxonomic order, (4) sample size, when available, (5) ovariole number, and (6) additional notes (e.g. for eusocial insects, whether the observation was made in a reproductive or non-reproductive individual). This dataset is made publically available at Dryad (doi:10.5061/dryad.59zw3r253).

Ovariole number was recorded as either an average with deviations, a range, or a single total value. When multiple types of data were available from a single publication, we recorded only a single type, with priority given to averages over ranges, and to both over single total values. Ovariole number was recorded as the total number of ovarioles per female, summing over both the left and right adult ovaries. When authors reported ovariole number from a single ovary, the total value was calculated by doubling the reported value. When authors described differences between the two ovaries, this information was recorded in an additional notes column.

For records of ovariole number that reported intraspecific variation in ovariole number, we calculated the percent difference as follows: if ovariole number was reported as a range, percent difference was calculated as the $100 * ((max - min)/median)$; if ovariole number was reported as an average with deviations, percent difference was calculated as $100 * ((2 * deviation)/mean)$. When independent observations of ovariole number for a given species were available across multiple published records, we calculated the percent difference as the $100 * ((max - min)/median)$ (Fig. S1).

Using this approach, we gathered 3355 records for ovariole number from 448 publications. A full list of publications is provided in the supplementary file 'ovariole_number_bibliography.pdf'. We matched the scientific names to additional taxonomic information using the software TaxReformer[1] and found additional taxonomic data for 3252 of the 3355 records. We verified that TaxReformer had found a valid match by comparing the originally recorded taxonomic order to the order populated by online databases, and removed 22 taxonomic records for which these values did not match. For all subsequent analyses, we also excluded observations made in non-reproductive individuals from eusocial species (workers), as well as two observations which represented significant outliers and could not be validated using additional sources or figures[2,3].

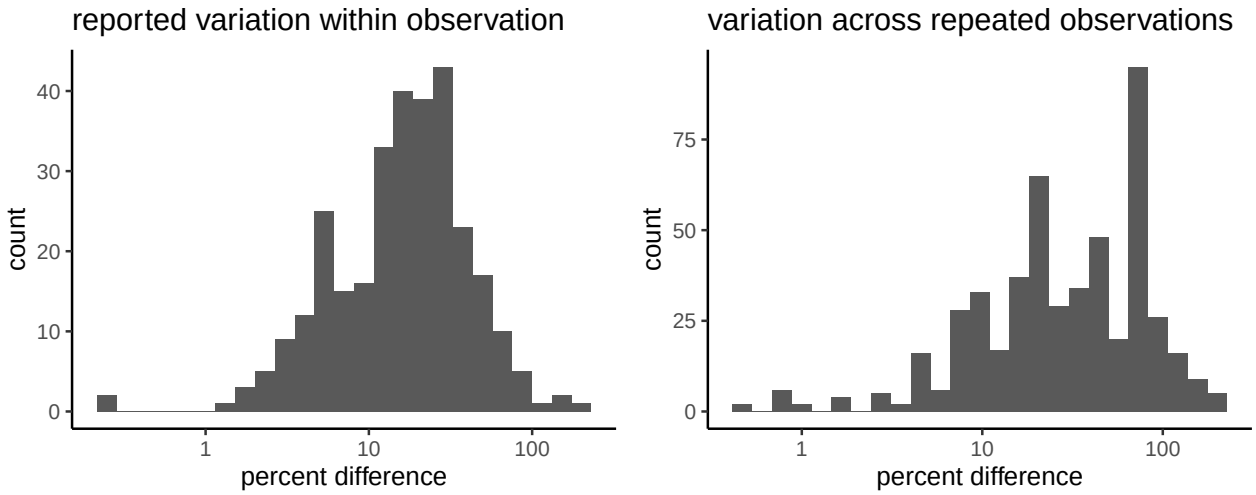

Figure S1: **Intraspecific variation in ovariole number.**

2 Phylogenetic trees

The analyses herein were performed using the insect phylogeny published in Church et al, 2019[4], unless otherwise specified. This phylogeny was constructed by combining ribosomal genetic data from 1726 insect genera, published originally in the SILVA database[5], with constrained, time-calibrated nodes for each insect order, published originally in Misof et al, 2014[6]. This phylogeny is enriched for insect genera with records in the egg trait dataset, and also has considerable overlap with the genera included in this ovariole number dataset (508 genera). For generalized least squares analyses and trait model comparisons, analyses were performed over a posterior distribution of trees associated with this published phylogeny[4].

For regressions involving body size data that were reported as insect family-level averages, we used the insect phylogeny published in Rainford et. al, 2014[7].

Analyses of Drosophilidae ovariole number, egg size, and body size were performed using a phylogeny newly assembled for this study. Published genetic data for 317 Drosophilidae species were retrieved from NCBI in June of 2019[8–16]. These data encompassed 41 gene regions including mitochondrial, nuclear, and ribosomal genes. When multiple sequences for a gene region were available from the same species, the one with the least amount of missing data was selected. Each gene region was aligned using the program MAFFT[17], model auto selected). Alignments were concatenated and trimmed to 3% occupancy across species using the program phyutlity[18]. Documentation including accession numbers, sequence files, and alignments are available in the supplementary directory 'https://github.com/shchurch/insect_ovariole_number_evolution_2020/phylogeny/Drosophilidae_sequences/'.

To the extent possible, sequence data were not curated beyond what was downloaded from NCBI, with the following exceptions: [1] two sequences labeled as 16S that did not align to other 16S sequences were removed manually. [2] COI sequences were trimmed to remove regions with large quantities of missing sites prior to alignment. [3] One species name (*D. albovittata*) was corrected for typographical error. [4] Sequences identified as *Drosophila crassifemur* were taxonomically corrected to *Scaptomyza crassifemur*[19].

Phylogenetic estimation of the Drosophilidae data were performed using RAxML (model GTRGAMMA), setting the split between Hawaiian *Drosophila* and *Scaptomyza* as the root of the tree[8,11]. The final tree was pruned to remove undescribed species (e.g. *Drosophila* nr *dorsigera*), and was time-calibrated using the R package ape, function chronos (default parameters, version 5.4.1)[20]. This tree is available in the supplementary file 'https://github.com/shchurch/insect_ovariole_number_evolution_2020/phylogeny/Drosophilidae_time_calibrated.tre'.

3 Phylogenetic regressions

3.1 Combining datasets

We combined the data we collected on total ovariole number with existing datasets of egg size and shape[21], insect lifetime fecundity and dry adult body mass[22–24], average adult body length per insect family[25], and several lineage-specific measures of adult body size[26–30].

Ovariole number and egg size[4] data were combined by matching records across datasets for the same insect species (Fig 2a). When multiple records existed for a given species, the dataset was randomly shuffled and a single matching record was selected. This variation across records for the same species was accounted for in regressions by reshuffling and matching records at each iteration of the analysis. We also matched records for insects in the same genus following the same reshuffling method, which allowed us to test whether results were robust with a larger sample size when an exact species match was not available (Fig. S2).

Average adult body length per insect family[25] was matched to the average ovariole number for the corresponding families (Fig. S5). The Rainford et al, 2016[25] dataset contains a small number of average adult body lengths at the order level (e.g. Strepsiptera), which were matched to their equivalent group in the ovariole number dataset. To test the effect of uncertainty in the estimated average ovariole number on our results, the dataset for each family was downsampled by half at each iteration of the regression analysis.

Ovariole number, egg volume, lifetime fecundity, and adult body mass[22–24] were combined by matching records at the species level and genus level, using the same method as described above (Figs. 2b, 3, and S4). We excluded one value from this dataset which appeared to include a typographical error for lifetime fecundity (Hymenoptera: Trichogrammatidae, lifetime fecundity recorded as 0.1[22]).

Several lineage-specific measurements for body size were matched to the ovariole number and egg size datasets, as follows: Drosophilidae thorax length[29] was matched at the species level (Fig. 2c), Orthoptera body length[28] was matched at the genus level (Fig. 2d), Hymenoptera mesosoma width[27] was matched at the genus level, and Curculonoidea elytra length[26] was matched at the genus level (Fig. S7).

3.2 Phylogenetic Generalized Least Squares (PGLS) analyses

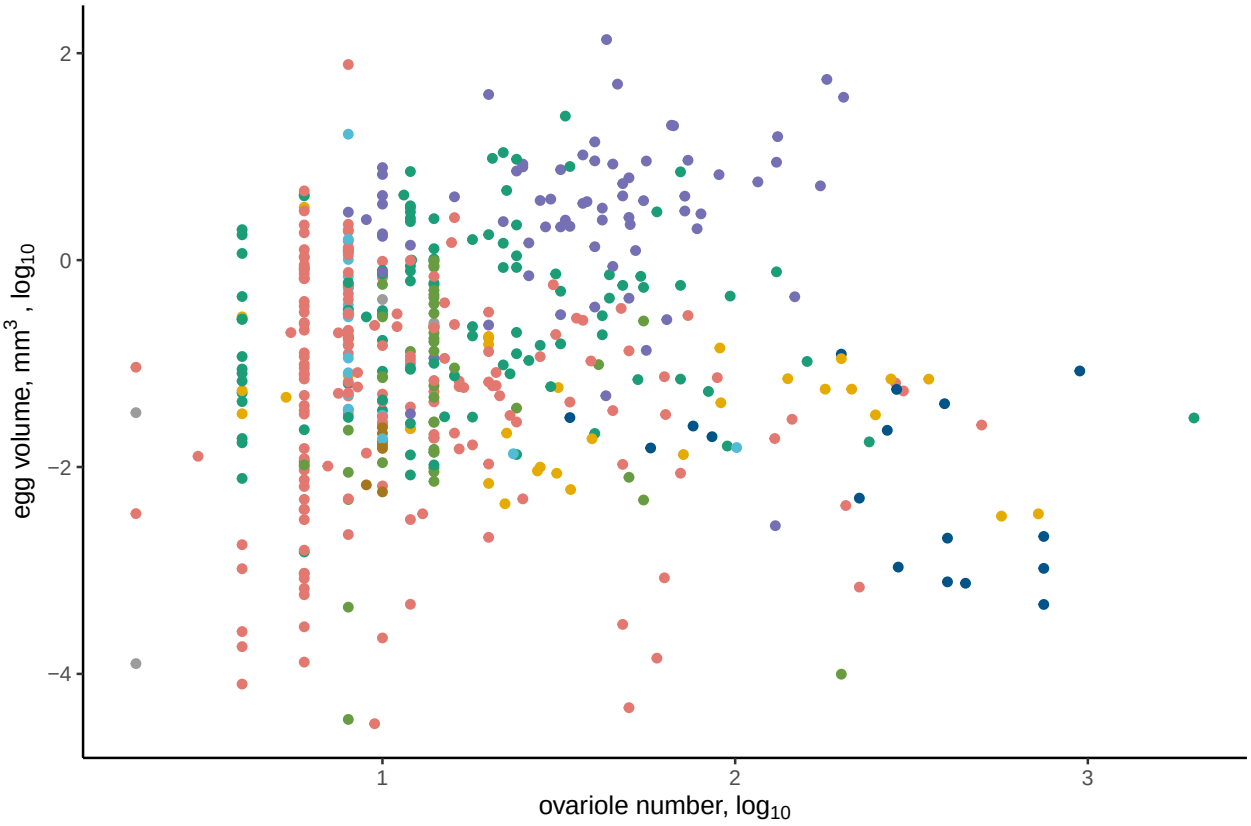

Figure S2: **Egg volume vs ovariole number, matching records at the genus level.**

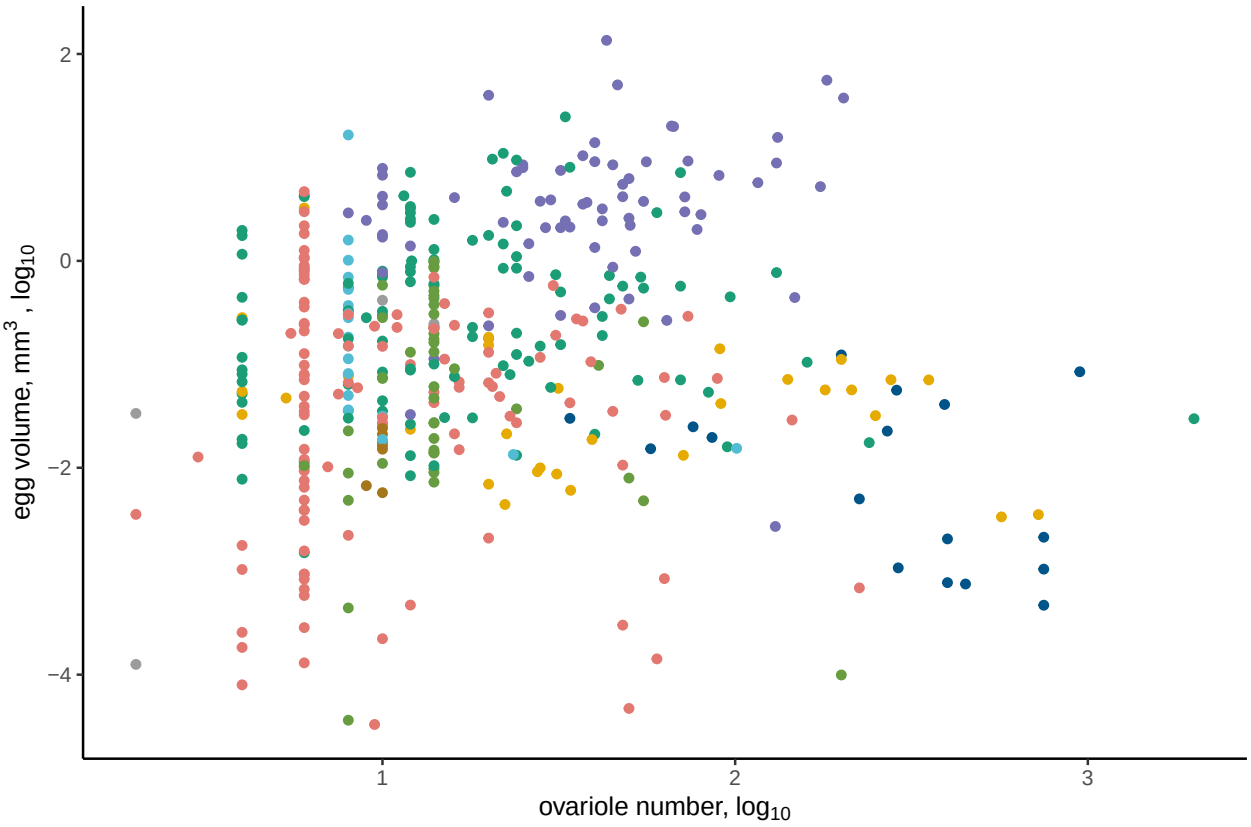

Figure S3: **Egg volume vs ovariole number, matching records at the genus level, excluding records from families with eusocial insects.**

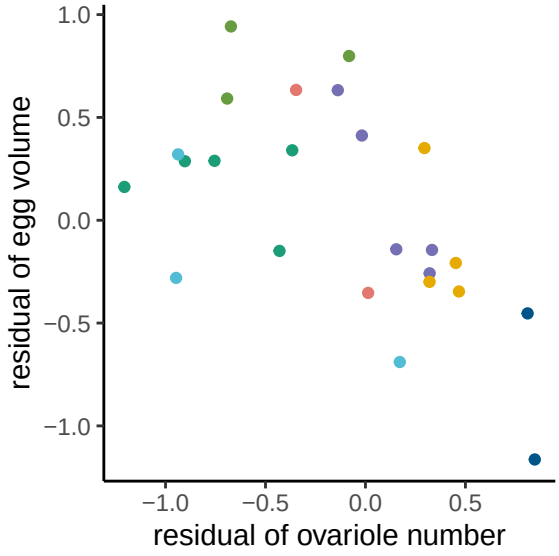

Figure S4: **Egg volume vs ovariole number, phylogenetic residuals to dry adult body mass, matching records at the species level.**

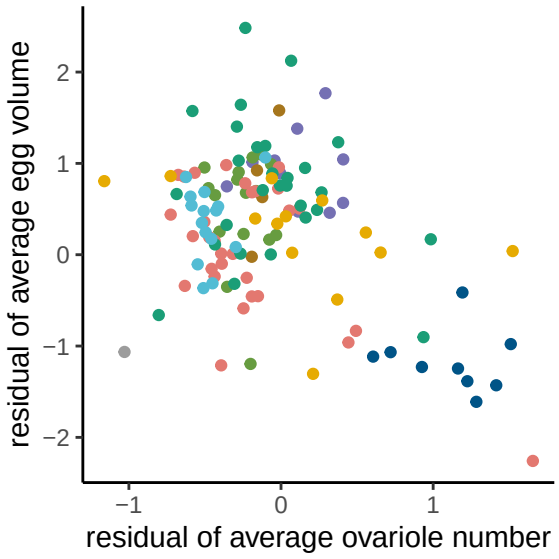

Figure S5: **Family average egg volume vs ovariole number, phylogenetic residuals to adult body length.**

We ran each Phylogenetic Generalized Least Squares (PGLS) regression over the Maximum Clade Credibilty (MCC) tree. For each regression, we also repeated each PGLS analysis 1000 times, accounting for phylogenetic and phenotypic uncertainty, using the R packages ape (version 5.4.1)[20] and nlme (version 3.1.151)[31]. In these analyses we used a Brownian Motion based covariance matrix for traits.

For regressions using data matched across species or genera, we reshuffled and matched records at each iteration to account for variation across records for the same taxon. For regressions on family-level average data, we recalculated the average ovariole number per insect family, downsampling the representation for each family by half. No posterior distribution was available with the previously published family level phylogeny[7].

To account for body size, we calculated the phylogenetic residuals[32] of each trait to body size, and then compared the evolution of these residuals using a PGLS regression.

For regressions of egg size and ovariole number when accounting for adult body size, we compared the results of our regression analyses to distributions estimated using simulated data under alternative hypotheses. We fit a Brownian motion model to the phylogenetic residuals of egg size and body size (R package geiger, version 2.0.7)[33], and then used the parameters of this fitted model to simulate new datasets (R package phylolm, version 2.6.2)[34]. We performed this resimulation using the datasets of egg size and body length at the family level, and egg size and body mass at the genus level. We simulated 1000 datasets each under two hypotheses: no correlation (slope=0) and a strong negative correlation (slope=-1). We performed the regressions as described above and compared the distribution of p-values and slopes to values from regressions on observed data.

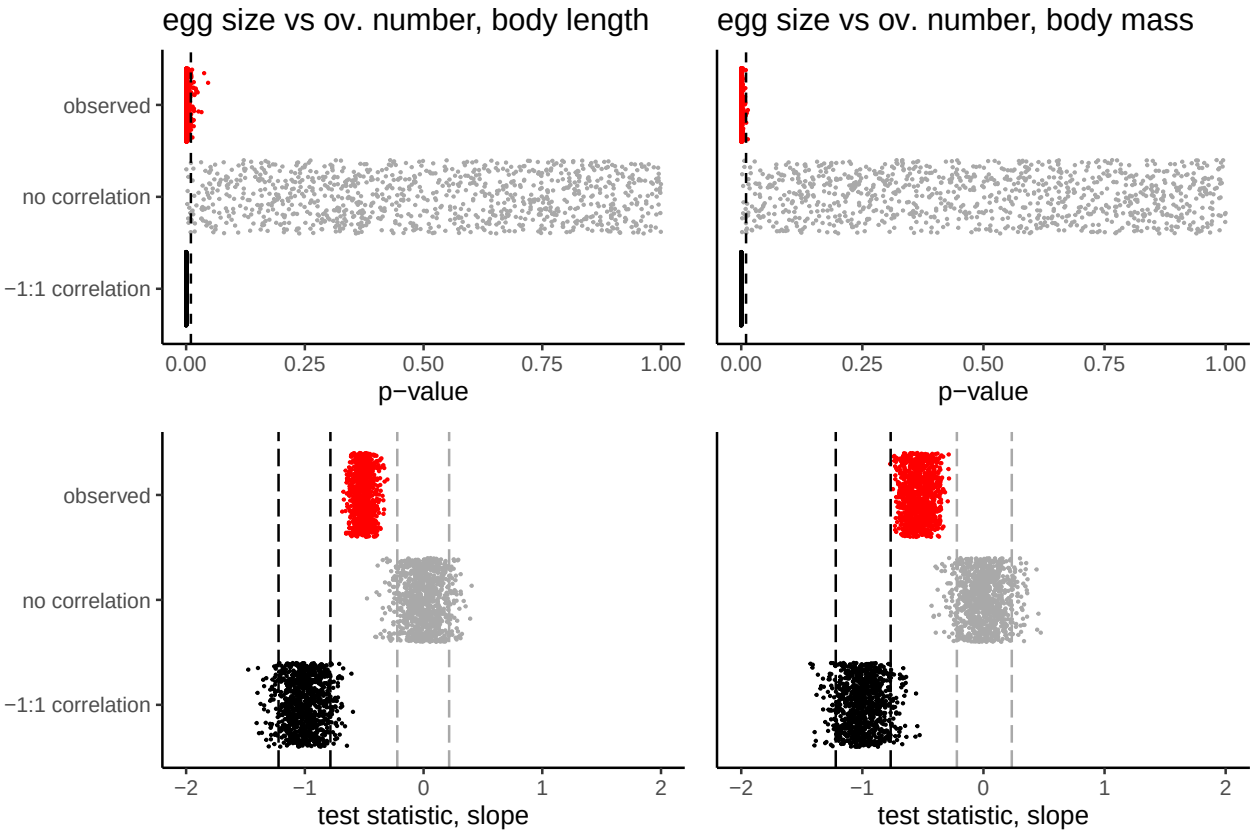

Figure S6: **Using simulated data to test alternative hypotheses of evolutionary relationships.** Top row, distributions of p-values over 1000 replicate regressions, dashed black line indicates threshold of 0.01. Bottom row, distribution of estimated slopes between egg size and ovariole number, dashed lines indicate 95% interval of simulated distributions. Left, comparing egg size and ovariole number, accounting for body length at the family level. Right, comparing egg size and ovariole number, accounting for body mass at the genus level. The slope of regressions on observed egg size and ovariole number (red) is more negative than we would expect to observe by chance, as assessed by comparing to data simulated with no evolutionary correlation (gray), but also not within the range that would be expected under an strong negative correlation (black). Red=observed values, gray=simulated with no correlation, black=simulated with a -1:1 correlation. n=1000 regressions.

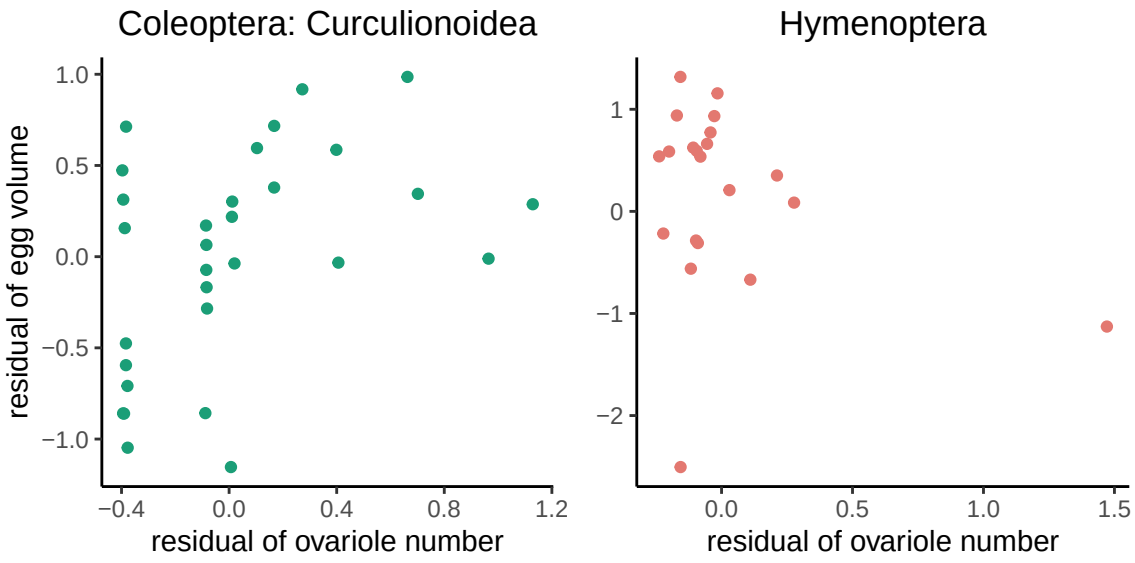

Figure S7: **Additional lineage-specific comparisons of egg volume vs ovariole number, phylogenetic residuals to body size, matching records at the genus level.** Weevils (Curculionoidea, left) were measured using elytra length and wasps (Hymenoptera, right) were measured using mesosoma width.

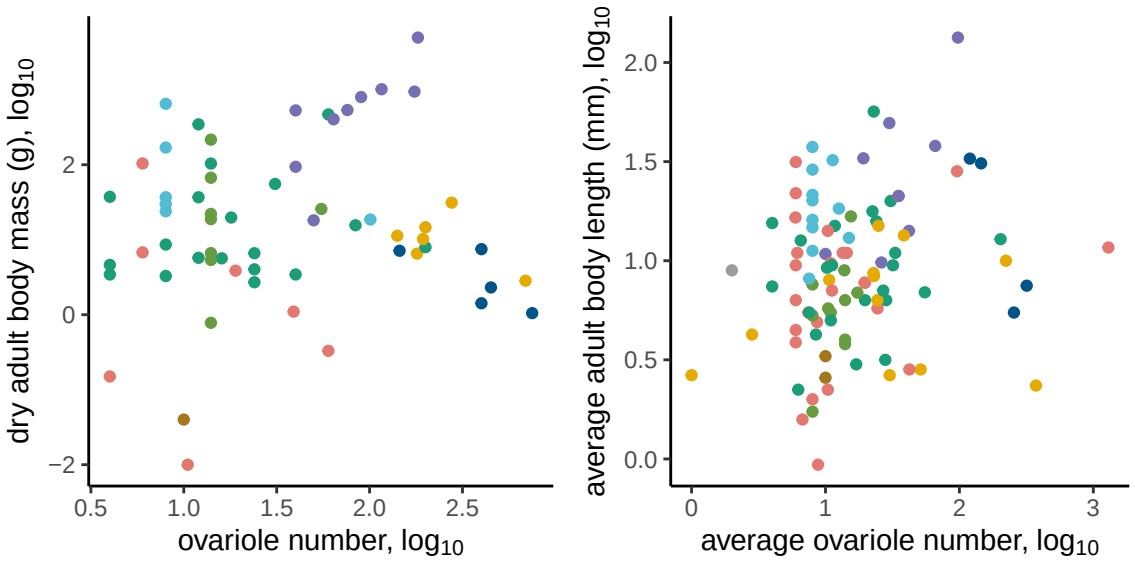

Figure S8: **Adult body size vs ovariole number.** Adult body mass, matching records at the genus level (left), and family-level average adult body length (right).

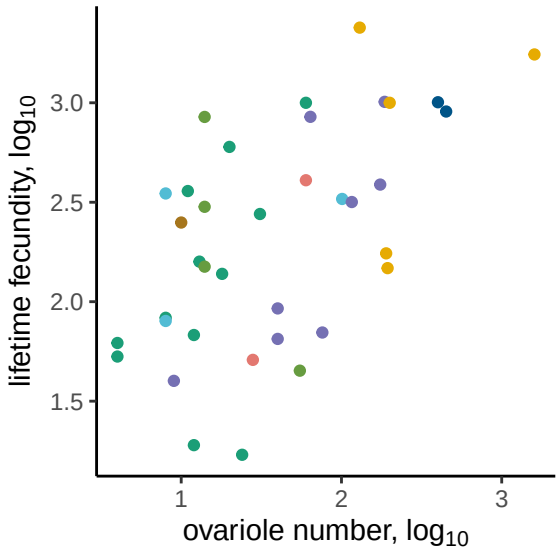

Figure S9: **Lifetime fecundity vs ovariole number, matching records at the species level.**

Table S1: Results of PGLS analysis of ovariole number and egg size across a posterior distribution. The 'data match' columns describes how observations were matched across datasets, e.g. matching records for the same species, genera, or using family-level averages.

analysis	data match	slope	MCC p-value	num. sig. / 1000	taxa
ovariole number vs egg volume	species	-0.426 – -0.082	0.195	43	306
ovariole number vs egg volume	genus	-0.356 – -0.128	0.066	470	482
ovariole number vs egg volume, residuals to body mass	species	-0.646 – -0.333	0.003	833	24
ovariole number vs egg volume, residuals to body mass	genus	-0.769 – -0.284	0.003	995	61
ovariole number vs egg volume, residuals to body length	family average	-0.685 – -0.304	<0.001	966	98

Table S2: Results of PGLS analysis of ovariole number and egg size across a posterior distribution.

analysis	data match	slope	MCC p-value	num. sig. / 1000	taxa
Drosophilidae ovariole number vs egg volume, residuals to thorax length	species	-0.814 – -0.799	<0.001	1000	30
Orthoptera ovariole number vs egg volume, residuals to body length	genus	-0.315 – 0.379	0.485	0	40
Curculionoidea ovariole number vs egg volume, residual to elytra length	genus	-0.293 – 0.633	0.384	0	30
Hymenoptera ovariole number vs egg volume, residuals to mesosoma width	genus	-2.131 – -0.288	0.139	13	21

Table S3: Results of PGLS analysis of ovariole number and body size across a posterior distribution.

analysis	data match	slope	MCC p-value	num. sig. / 1000	taxa
ovariole number vs body length	species	0.025 – 0.208	0.618	0	24
ovariole number vs body mass	genus	0.095 – 0.299	0.546	0	61
ovariole number vs body mass	family average	0.123 – 0.177	0.031	29	98
Drosophilidae ovariole number vs thorax length	species	0.223 – 0.223	0.031	0	30
Orthoptera ovariole number vs body length	genus	0.132 – 0.450	0.001	993	40
Curculionoidea ovariole number vs elytra length	genus	-0.211 – 0.257	0.917	0	30
Hymenoptera ovariole number vs mesosoma width	genus	-0.112 – 0.355	0.482	0	21

Table S4: Results of PGLS analysis of ovariole number and fecundity across a posterior distribution.

analysis	data match	slope	MCC p-value	num. sig. / 1000	taxa
ovariole number vs lifetime fecundity	species	0.324 – 0.542	0.011	311	37
ovariole number vs lifetime fecundity	genus	-0.275 – 0.601	0.002	267	65

4 Evolution of nurse cells

4.1 Combining datasets

We used the descriptions of the mode of oogenesis recorded by Büning[35]. This author catalogued the ovary morphology for 136 insect genera, categorizing them into four modes: those without nurse cells (panoistic), with nurse cells adjacent to each clonally related, developing oocyte (polytrophic meroistic), with all nurse cells located in the germarium (telotrophic meroistic), and a unique mode of oogenesis reported only in Strepsiptera (reduced polytrophic meroistic ovaries).

Of the 136 genera observed by Büning, 70 are represented in the phylogeny used here[4]. Another 36 come from families or orders that have representative genera in the phylogeny, and within which all observations have the same recorded mode of oogenesis, when more than one was recorded. Therefore, we used a substitute genus as the phylogenetic tip for these 36 groups, bringing the total overlap between dataset and phylogeny to 106 taxa.

4.2 Reconstructing evolutionary shifts in oogenesis mode

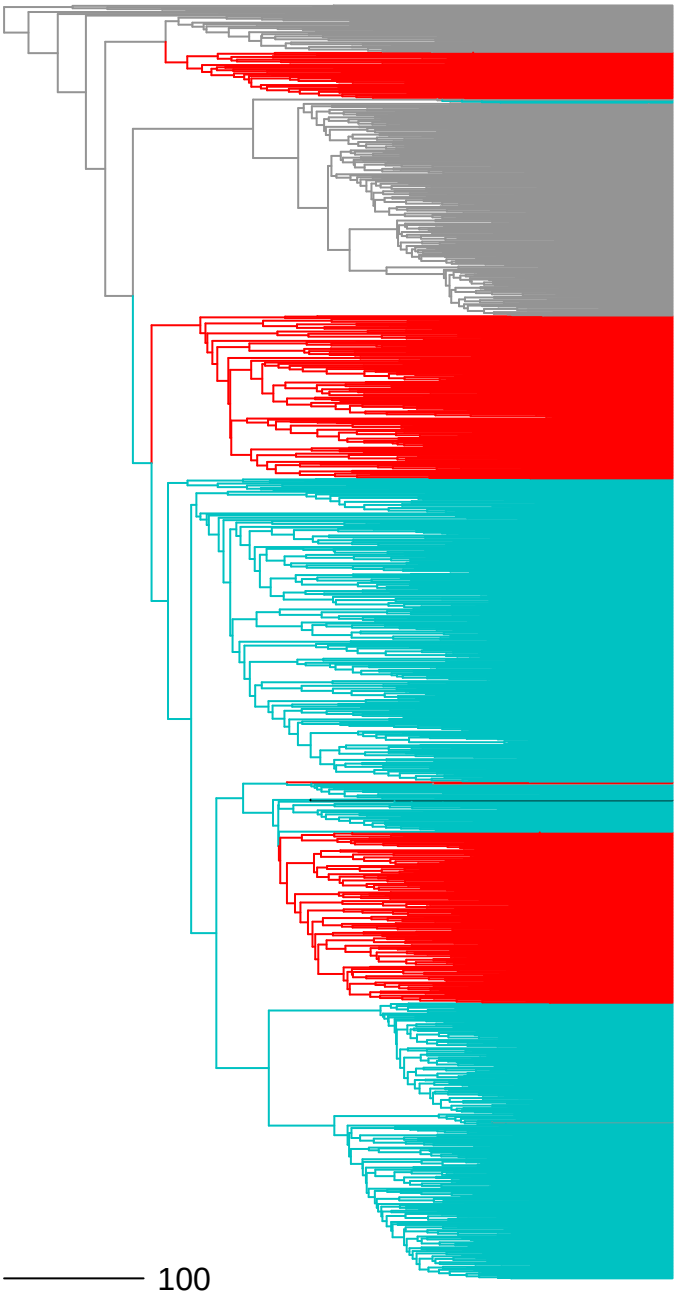

Figure S10: **Ancestral state reconstruction of oogenesis mode, full phylogeny.** Scale bar indicates 100 million years. Gray = panoistic, red = telotrophic meroistic, cyan = polytrophic meroistic, black = unique meroistic mode found in Strepsiptera.

Using these 106 records for ovary type, we reconstructed the ancestral state at each node of the published phylogeny of 1705 insect genera using an equal-rates model that allows for missing data (Fig. S10, R package corHMM, version 1.22[36] function rayDISC, node.states = 'marginal').

4.3 Oogenesis mode model comparison

Table S5: Average corrected AIC (AICc) value from model comparison

analysis name	BM1	BMS	OU1	OUM
ovariole number	477.20195	473.03372	479.22592	482.42889
egg volume	3295.74949	3281.71001	3297.75729	3299.52446
egg aspect ratio	-1486.86444	-1506.89208	-1484.85630	-1483.01934
egg asymmetry	-763.10658	-785.44797	-808.70150	-810.07385
egg curvature	62.36224	35.70801	63.46489	64.20869

Table S6: Results of model comparison analysis over posterior distribution, showing the number of iterations out of 100 where the difference in model fit (ΔAICc) was greater than 2.

analysis name	BMS vs. BM1	OU1 vs. BM1	OUM vs. BM1	OUM vs. OU1	taxa
ovariole number	90	0	0	0	506
egg volume	100	0	0	0	1567
egg aspect ratio	100	0	0	0	1488
egg asymmetry	100	100	100	20	844
egg curvature	100	1	1	1	781

Using the ancestral state reconstruction of evolutionary shifts in the mode of oogenesis, we inferred the most likely mode of oogenesis for all nodes and unobserved extant tips in the phylogeny (Fig. S10). We then compared the fit of models of trait evolution that take into account these shifts in oogenesis mode against those that do not. These comparisons were performed with the R package OUwie (version 1.57)[37].

Each analysis compared four models of evolution: single-rate Brownian Motion (BM1), multi-rate Brownian Motion (BMS), single-optimum Ornstein-Uhlenbeck (OU1), and an Ornstein-Uhlenbeck model with different optima for each mode of oogenesis (OUM).

These comparisons were repeated 100 times over a posterior distribution of trees. At each iteration we selected a random representative trait record for each genus in the phylogeny, when multiple records were available.

5 Modeling rate of ovariole number change

5.1 Parametric bootstrap of Brownian Motion model

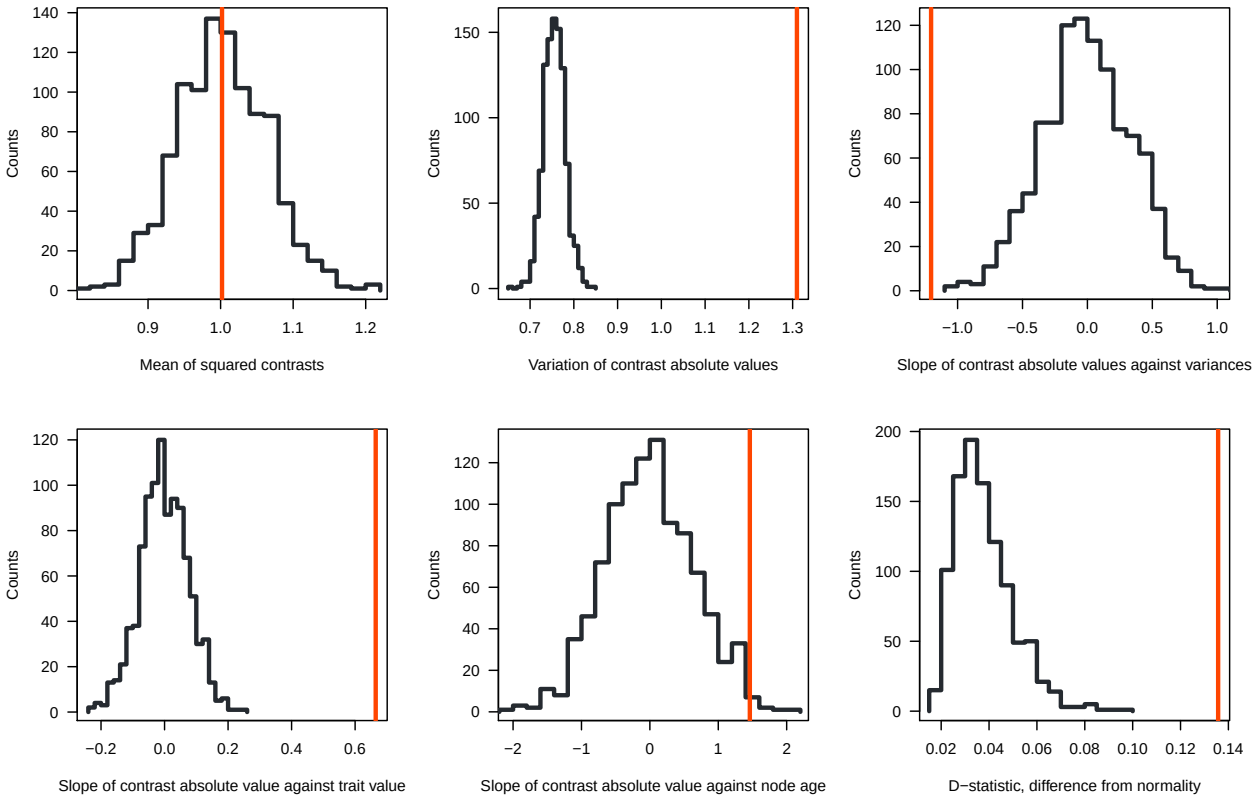

Figure S11: **Bootstrap analysis of Brownian Motion model for ovariole number evolution, using the R package arbutus.** In each panel the red line represents the observed value and the black distribution represents the bootstrap simulation. See Section 5 for details on each parameter.

We evaluated the fit of a Brownian Motion (BM) model for ovariole number evolution using the R package arbutus (version 0.1[38], Fig. S11). In this approach, a BM model is fit to the data (R package geiger, version 2.0.7)[33], and the resulting parameters of the model are used to simulate 1000 new datasets. Six statistical parameters are used to compare the phylogenetic contrasts of the observed data to the simulated data, and their interpretations are as follows[38]:

1. *Mean of squared contrasts.* The rate of evolution of ovariole number can be well estimated by the Brownian Motion model (the observed value falls within the null distribution).
2. *Coefficient of variation of the absolute value of the contrasts.* There is substantially more variation in contrasts than expected by chance, indicating heterogeneity in the rate of evolution beyond what a single-rate Brownian Motion model predicts (the observed value falls well outside the null distribution).
3. *Slope of a linear model fitted to the absolute value of the contrasts against their expected variances.* Contrasts are larger than expected on short branches in the phylogenetic tree, resulting in a negative slope. This could be explained by error in estimation of branch lengths.
4. *Slope of a linear model fitted to the absolute value of the contrasts against the ancestral state at the corresponding node.* The number of ovarioles is more correlated with contrast values than would be expected by chance. Phylogenetic nodes with a low ovariole number experience lower rates of evolution.

5. *Slope of a linear model fitted to the absolute value of the contrasts against node depth.* Contrast values are not correlated with time, falling within the null distribution. Therefore the rate of ovariole number change is not increasing or decreasing over time.
6. *The D statistic from a Kolmogorov-Smirnov test comparing the distribution of contrasts to an expected normal distribution.* The data do not fit a normal distribution of contrasts well, suggesting there are likely non-Brownian motion based processes at play (e.g. jump-diffusion processes).

5.2 Assessing rate heterogeneity

Given the result that our dataset contains substantial rate heterogeneity, we identified regions of the tree with high and low rates of ovariole number evolution using the software BAMM (version 2.5.0)[39]. For this analysis, we calculated the average ovariole number for each genus in the insect phylogeny[4]. Average ovariole number was $\log_{10}$ transformed, and the tree was filtered to include only tips for which there were corresponding ovariole number data (sample size = 508). We used the R package BAMMtools (version 2.1.7)[40] to select priors, and ran BAMM for the maximum number of generations ($2 * 10^9$), sampling every 10^6 generations.

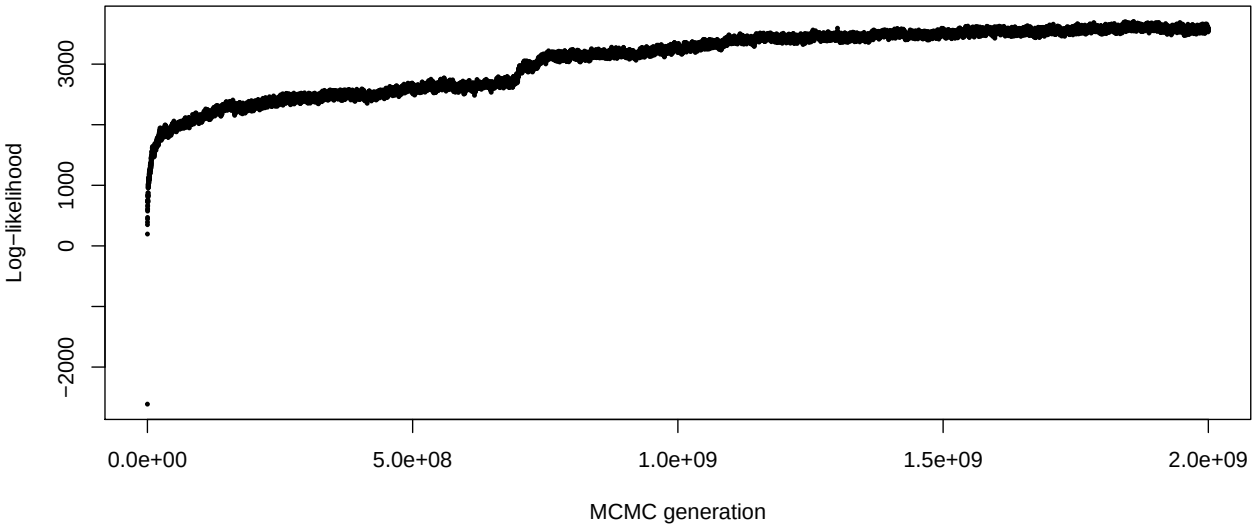

Figure S12: Convergence of trait diversification rate analysis

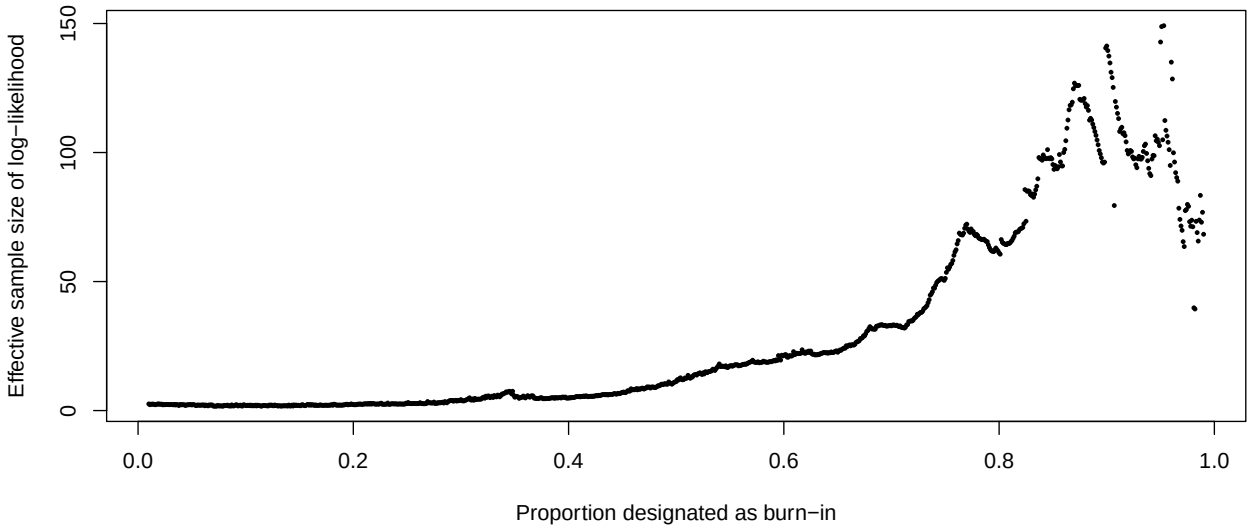

Figure S13: **Comparison of burn-in proportions.** The burn-in proportion that maximized the effective size was used in subsequent analyses.

Convergence was evaluated both visually (Fig. S12) and numerically by comparing the effective sample size for number of shifts and log-likelihood to the standard recommended by the software (>200). We determined the most appropriate burn-in proportion to use by finding the maximum effective sample size of the log-likelihood across an array of possible burn-in proportions (Fig. S13). Running BAMM for the maximum possible number of generations and selecting the optimum burn-in (Fig. S13) resulted in an effective size for the number of shifts of 482.51, and for log-likelihood of 149.15. Repeated BAMM analyses showed similar distributions of high and low rate regimes, indicating the implications for ovariole number evolution are robust to uncertainty in rate estimates. See Supplemental Methods Section 5.2 for details.

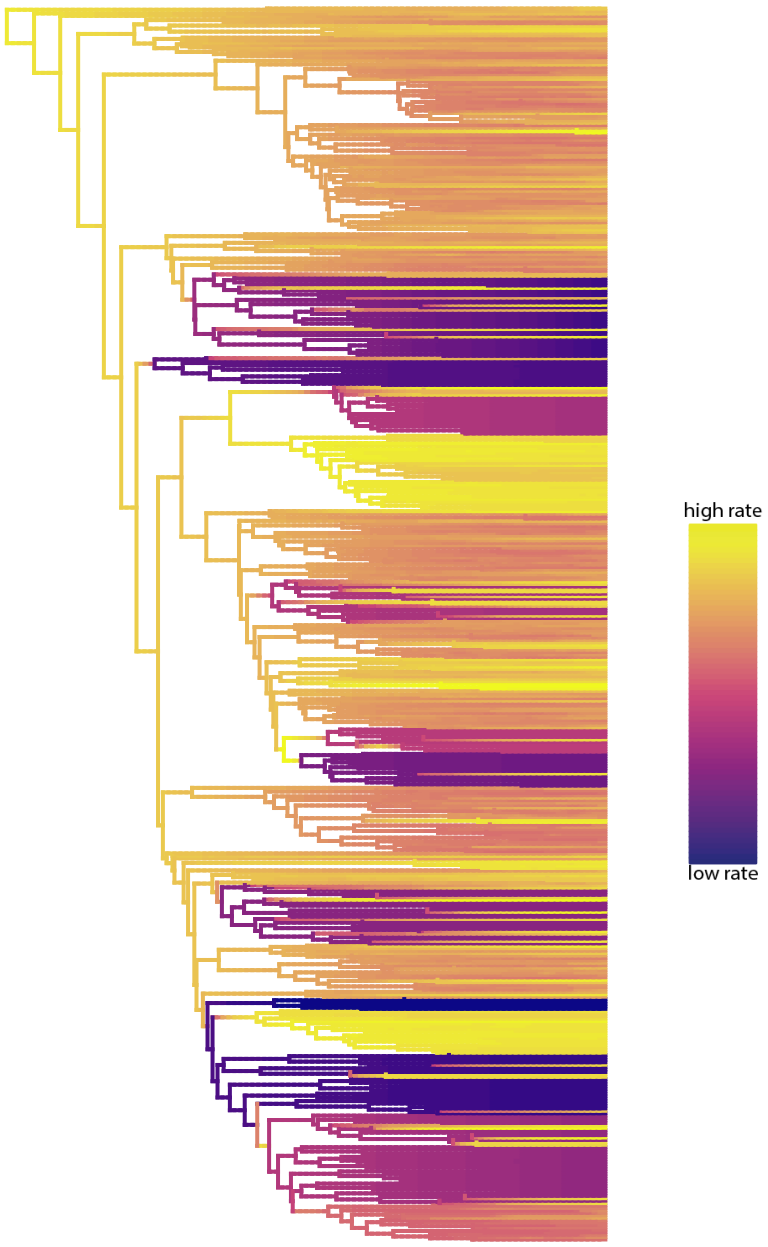

Figure S14: **Best rate shift configuration from BAMM trait diversification analysis on ovariole number.** Purple = low rate of evolution, yellow = high rate of evolution.

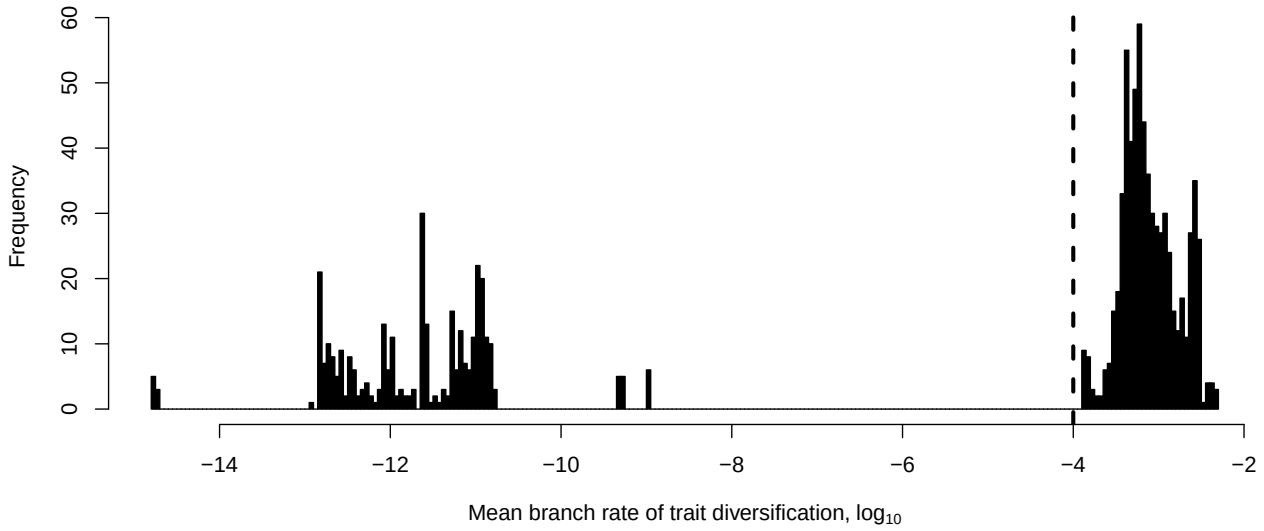

Figure S15: **Distribution of trait diversification rates.** Dotted line shows threshold used to assigned rate regimes.

The best configuration of rate shift regimes shows multiple independent clades with very low rates of evolution (Fig. S14). Visualizing the distribution of mean rates along branches revealed a discontinuous distribution, with one peak at a moderate rate of evolution and several clusters at extremely low rates, separated from the first peak by over six orders of magnitude (Fig. S15). We used this visualization to establish a threshold (10^{-4}) for assigning a binary rate regime to each node in the phylogeny, categorizing them as above (variable) or below (invariant) a threshold that separates these two peaks.

5.3 Rate model comparison

We tested whether a BM model of evolution that incorporates the binary state (variable or invariant) as independent rate regimes can better explain the distribution of ovariole numbers than a single rate BM model, by comparing model fit using the R package OUwie (version 2.5)[37]. We find that a multi-rate model is significantly favored over a single-rate model (Δ AICc 1770.93).

5.4 Comparing rates of trait diversification

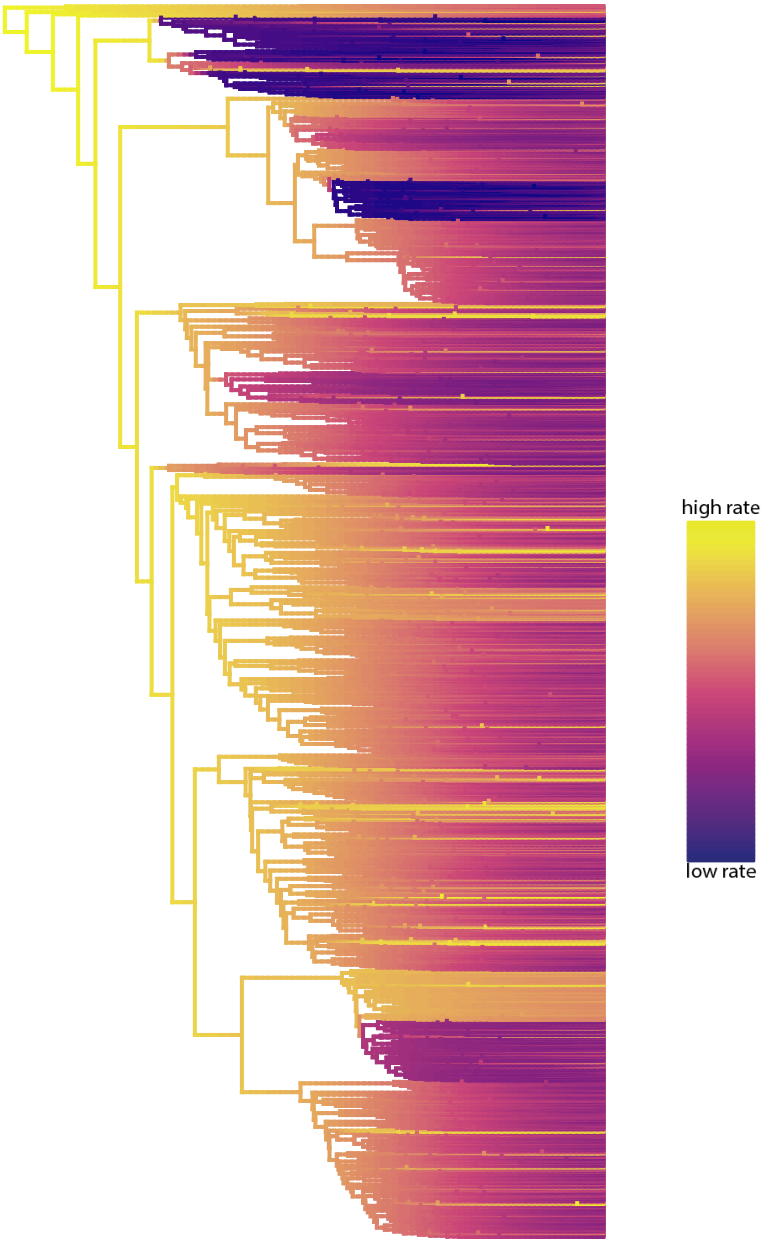

Figure S16: **Best rate shift configuration from BAMM trait diversification analysis on egg volume.** Purple = low rate of evolution, yellow = high rate of evolution.

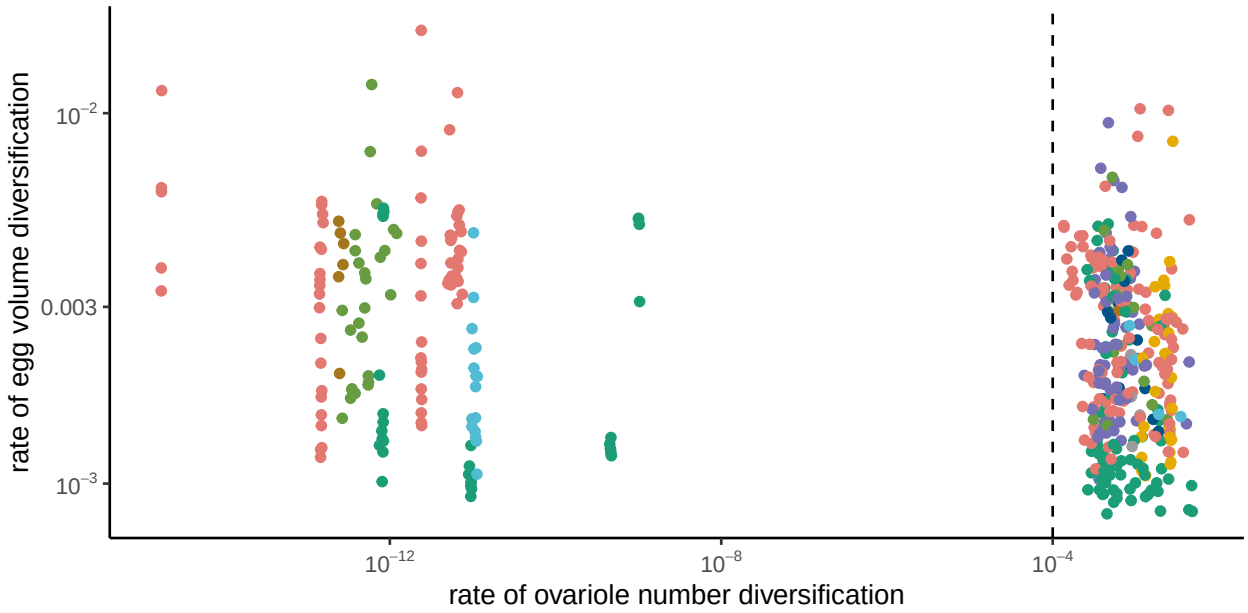

Figure S17: **Rates of trait diversification of egg volume and ovariole number.** Points are colored by phylogenetic groups shown in Fig 1a. Dotted line shows threshold used to assigned rate regimes.

We assessed the rate of egg volume diversification across insects using the same method of assessing rate heterogeneity as described in Section 5.2 (Fig. S16). This analysis converged in $7 * 10^9$ generations (the effective size for the number of shifts and log-likelihood were >200, 670.2 and 753.42 respectively). We compared the correlation between the rates of trait diversification for ovariole number and egg volume by matching the mean rate predicted for each insect genus (the tips of the phylogeny from the BAMM analyses, Fig. S17).

References

1. Medeiros, B. A. S. de. TaxReformer. https://github.com/brunoasm/TaxReformer (2019).

2. Su, X. H. *et al.* Testicular development and modes of apoptosis during spermatogenesis in various castes of the termite *Reticulitermes labralis* (Isoptera: Rhinotermitidae). *Arthropod Structure and Development* **44**, 630–638 (2015).

3. Hernandez, L. C., Fajardo, G., Fuentes, L. S. & Comoglio, L. Biology and reproductive traits of *Drymoea veliterna* (druce, 1885) (lepidoptera: Geometridae). *Journal of Insect Biodiversity* **5**, 1–9 (2017).

4. Church, S. H., Donoughe, S., Medeiros, B. A. de & Extavour, C. G. Insect egg size and shape evolve with ecology but not developmental rate. *Nature* **571**, 58–62 (2019).

5. Yilmaz, P. *et al.* The SILVA and "all-species Living Tree Project (LTP)" taxonomic frameworks. *Nucleic Acids Research* **42**, 643–648 (2014).

6. Misof, B. *et al.* Phylogenomics resolves the timing and pattern of insect evolution. *Science* **346**, 763–767 (2014).

7. Rainford, J. L., Hofreiter, M., Nicholson, D. B. & Mayhew, P. J. Phylogenetic distribution of extant richness suggests metamorphosis is a key innovation driving diversification in insects. *PLoS One* **9**, e109085 (2014).

8. Katoh, T., Izumitani, H. F., Yamashita, S. & Watada, M. Multiple origins of Hawaiian drosophilids: Phylogeography of *Scaptomyza* Hardy (Diptera: Drosophilidae). *Entomological Science* **20**, 33–44 (2017).

9. Magnacca, K. N. & Price, D. K. Rapid adaptive radiation and host plant conservation in the Hawaiian picture wing *Drosophila* (Diptera: Drosophilidae). *Molecular Phylogenetics and Evolution* **92**, 226–242 (2015).

10. Lapoint, R. T., Magnacca, K. N. & O'Grady, P. M. Phylogenetics of the antopocerus-modified tarsus clade of Hawaiian *Drosophila*: Diversification across the Hawaiian islands. *PLoS One* **9**, (2014).

11. O'Grady, P. M. *et al.* Phylogenetic and ecological relationships of the Hawaiian *Drosophila* inferred by mitochondrial DNA analysis. *Molecular Phylogenetics and Evolution* **58**, 244–256 (2011).

12. Lapoint, R. T., Gidaya, A. & O'Grady, P. M. Phylogenetic relationships in the spoon tarsus subgroup of Hawaiian *Drosophila*: Conflict and concordance between gene trees. *Molecular Phylogenetics and Evolution* **58**, 492–501 (2011).

13. Bonacum, J., O'Grady, P. M., Kambysellis, M. & DeSalle, R. Phylogeny and age of diversification of the planitibia species group of the Hawaiian *Drosophila*. *Molecular Phylogenetics and Evolution* **37**, 73–82 (2005).

14. O'Grady, P. M. & Zilversmit, M. Phylogenetic relationships within the *Drosophila* haleakalae species group inferred by molecular and morphological characters (diptera: Drosophilidae). *Bishop Museum Bulletin In Entomology* **12**, 117–134 (2004).

15. Lapoint, R. T., O'Grady, P. M. & Whiteman, N. K. Diversification and dispersal of the Hawaiian Drosophilidae: The evolution of *Scaptomyza*. *Molecular Phylogenetics and Evolution* **69**, 95–108 (2013).

16. Baker, R. H. & DeSalle, R. Multiple sources of character information and the phylogeny of Hawaiian drosophilids. *Systematic Biology* **46**, 654–673 (1997).

17. Katoh, K. & Standley, D. M. MAFFT multiple sequence alignment software version 7: Improvements in performance and usability. *Molecular Biology and Evolution* **30**, 772–780 (2013).

18. Smith, S. A. & Dunn, C. W. Phyutility: A phyloinformatics tool for trees, alignments and molecular data. *Bioinformatics* **24**, 715–716 (2008).

19. O'Grady, P., Bonacum, J., DeSalle, R. & Do Val, F. The placement of *Engiscaptomyza*, *Grimshawomyia*, and *Titanochaeta*, three clades of endemic Hawaiian Drosophilidae (Diptera). *Zootaxa* **159**, 1–16 (2003).

20. Paradis, E., Claude, J. & Strimmer, K. APE: Analyses of phylogenetics and evolution in R language. *Bioinformatics* **20**, 289–290 (2004).

21. Church, S. H., Donoughe, S., Medeiros, B. A. de & Extavour, C. G. A dataset of egg size and shape from more than 6,700 insect species. *Scientific Data* **6**, 1–11 (2019).

22. Gilbert, J. D. J. *PhD Thesis*: The evolution of parental care in insects. (University of Cambridge, 2007).

23. Gilbert, J. D. & Manica, A. Parental care trade-offs and life-history relationships in insects. *The American Naturalist* **176**, 212–226 (2010).

24. Gilbert, J. D. J. Insect dry weight: Shortcut to a difficult quantity using museum specimens. *Florida Entomologist* **94**, 964–970 (2011).

25. Rainford, J. L., Hofreiter, M. & Mayhew, P. J. Phylogenetic analyses suggest that diversification and body size evolution are independent in insects. *BMC Evolutionary Biology* **16**, 8 (2016).

26. Iwata, K. Large-sized eggs in Curculionoidea (Coleoptera). *Research Bulletin of Hyogo Agricultural College* **7**, 43–45 (1966).

27. Iwata, K. & Sakagami, S. F. Gigantism and dwarfism in bee eggs in relation to the mode of life, with notes on the number of ovarioles. *Japanese Journal of Ecology* **16**, 4–16 (1966).

28. Waloff, N. Number and development of ovarioles of some Acridoidea (Orthoptera) in relation to climate. *Physiologia Comparata et Oecologia* vol. 3 370–390 (1954).

29. Starmer, W. T. *et al.* Phylogenetic, geographical, and temporal analysis of female reproductive trade-offs in Drosophilidae. *Evolutionary Biology* **33**, 139–171 (2003).

30. Reinhardt, K., Köhler, G., Maas, S. & Detzel, P. Low dispersal ability and habitat specificity promote extinctions in rare but not in widespread species: The Orthoptera of Germany. *Ecography* **28**, 593–602 (2005).

31. Pinheiro, J., Bates, D., DebRoy, S. & Sarkar, D. R Core Team (2014) nlme: Linear and nonlinear mixed effects models. R package version 3.1-117. *Available at http://cran.r-project.org/package=nlme* (2014).

32. Revell, L. J. Size-correction and principal components for interspecific comparative studies. *Evolution: International Journal of Organic Evolution* **63**, 3258–3268 (2009).

33. Harmon, L. J., Weir, J. T., Brock, C. D., Glor, R. E. & Challenger, W. GEIGER: Investigating evolutionary radiations. *Bioinformatics* **24**, 129–131 (2007).

34. Tung Ho, L. S. & Ané, C. A linear-time algorithm for Gaussian and non-gaussian trait evolution models. *Systematic Biology* **63**, 397–408 (2014).

35. Büning, J. *The insect ovary: Ultrastructure, previtellogenic growth and evolution.* (Springer Science & Business Media, 1994).

36. Beaulieu, J. M., O'Meara, B. C. & Donoghue, M. J. Identifying hidden rate changes in the evolution of a binary morphological character: The evolution of plant habit in campanulid angiosperms. *Systematic Biology* **62**, 725–737 (2013).

37. Beaulieu, J. M., Jhwueng, D.-C., Boettiger, C. & O'Meara, B. C. Modeling stabilizing selection: Expanding the Ornstein–Uhlenbeck model of adaptive evolution. *Evolution* **66**, 2369–2383 (2012).

38. Pennell, M. W., FitzJohn, R. G., Cornwell, W. K. & Harmon, L. J. Model adequacy and the macroevolution of angiosperm functional traits. *The American Naturalist* **186**, E33–E50 (2015).

39. Rabosky, D. L. Automatic detection of key innovations, rate shifts, and diversity-dependence on phylogenetic trees. *PLoS One* **9**, e89543 (2014).

40. Rabosky, D. L. *et al.* BAMM tools: An R package for the analysis of evolutionary dynamics on phylogenetic trees. *Methods In Ecology and Evolution* **5**, 701–707 (2014).